



Departamento de Física Teórica
Institute of Particle & Cosmos Physics (IPARCOS)
Universidad Complutense de Madrid



Determination of the $f_0(1370)$ from a novel dispersive analysis
of meson-meson scattering data

J. R. Peláez
A.Rodas
J.Ruiz de Elvira

Phys.Rev.Lett. 130 (2023) 5, 051902.

INT Workshop **Accessing and Understanding the QCD Spectra**
INT, Seattle, 20-25th March 2023

Supported by:



- $f_0(1370)$ candidate to complete the controversial scalar nonet above 1 GeV, Interesting for studies of lightest glueball and its mixing scheme.
- Main problem: Strong model dependence in determinations from data.

Use of specific models or parameterizations and dynamical assumptions

- PDG1984- Still called $\epsilon(1300)$
- PDG1986- $f_0(1300)$ “averages meaningless”
- PDG1988- $f_0(1400)$, crude estimates
- PDG1994- $f_0(1370)$ (due to Crystal Barrel)
- PDG1996 until 2021: Same T-matrix pole

(1200-1500)-i(150-250) MeV

- However, it is by far the worst determined scalar above 1 GeV. Moreover:

- *“Unfortunately, regardless of the year-long efforts, the scalar isoscalar spectrum is still not fully resolved: e.g. there is still an ongoing debate whether the $f_0(1370)$ exists or not ...”*

S. Ropertz, C. Hanhart and B. Kubis, Eur. Phys. J. C 78 (2018) no.12, 1000.

- *“However, the existence of $f_0(1370)$ is not beyond doubt”, and “As a conclusion, we do not consider the $f_0(1370)$ as established resonance”. E. Klempt and A. Zaitsev, Phys. Rept. 454 (2007), 1*

One of their main concerns is *“the absence of any measured $f_0(1370)$ phase motion*

Problems

- Not evident or present in original $\pi\pi \rightarrow \pi\pi$ experiments in the 70's but found in later models. (Froggat et al. Martin et al., Au, Morgan & Pennington, Kaminski, Lesniak & Maillet, Tornqvist, Janssen, Albaladejo & Oller, etc...)

- Data: extracted from $\pi N \rightarrow \pi\pi N$, assuming one pion exchange. Large systematic uncertainties and inconsistencies.

- Seen in other reactions (from pp scattering, heavier meson decays, etc), but widely different pole determinations

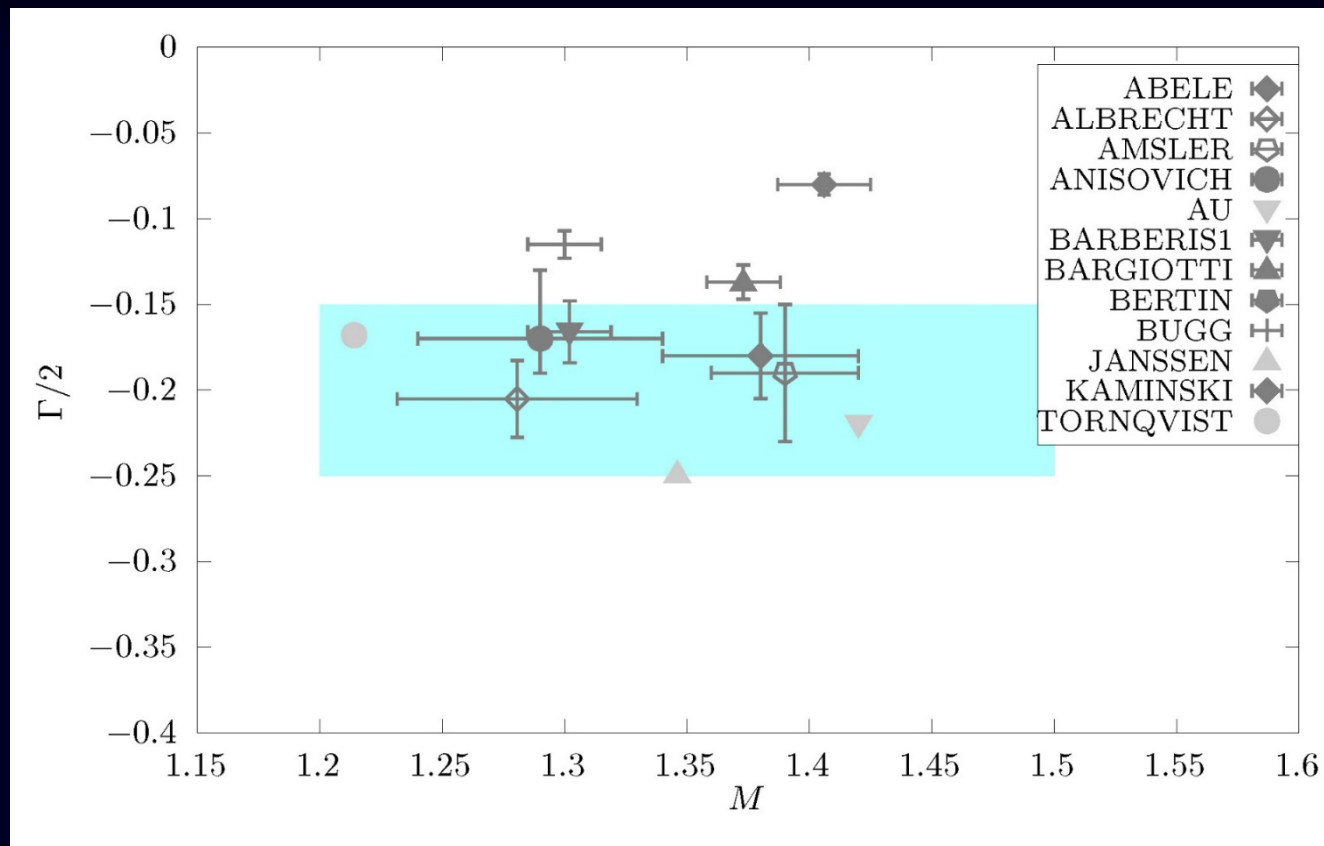
• Large model-dependences:

- naïve models often used for parameterizations and resonance poles
- Specific parameterizations with a priori relations between pole and residue
- Isobars
- Breit Wigners
- Choice of decay channels
- Multi body channels as quasi two body...
- “tree level dynamics” (resonances or lagrangian constants)

- PDG still quotes Breit-Wigner parameters. No partial widths. **Surprisingly...**

lists KK-mode masses > 1350 MeV whereas many in $\pi\pi$ -mode down to 1200 MeV

- PDG2021: T-matrix pole sample



Latest two entries@PDG:

$M-i \Gamma/2 = (1280.6 \pm 1.6 \pm 47.4) - i(205.2 \pm 1.7 \pm 20.7)$ ($p\bar{p}$, Crystal Barrell Collab. 2020)

$M-i \Gamma/2 = (1290 \pm 50) - i(170^{+20}_{-40})$ ($p\bar{p}$, πN , Anisovich & Sarantsev 2009)

Very recently:

$M-i \Gamma/2 = (1370 \pm 40) - i(195 \pm 20)$ (J/ψ , $p\bar{p}$, πN , ... Sarantsev, Denisenko, Thoma, Klempt PLB816 2021)

No evidence in J/ψ radiative decays (BESIII). Too tiny glueball component?

This work:

Data-Driven Forward Dispersion Relations (FDR)
Or partial-wave dispersion relations (Roy or Roy-Steiner)
(phase+elasticity)

Model independent constraints on data description
Enhanced precision



Analytic methods for the continuation to the
complex plane in the contiguous sheet
avoiding specific parameterizations
(only phase and elasticity)



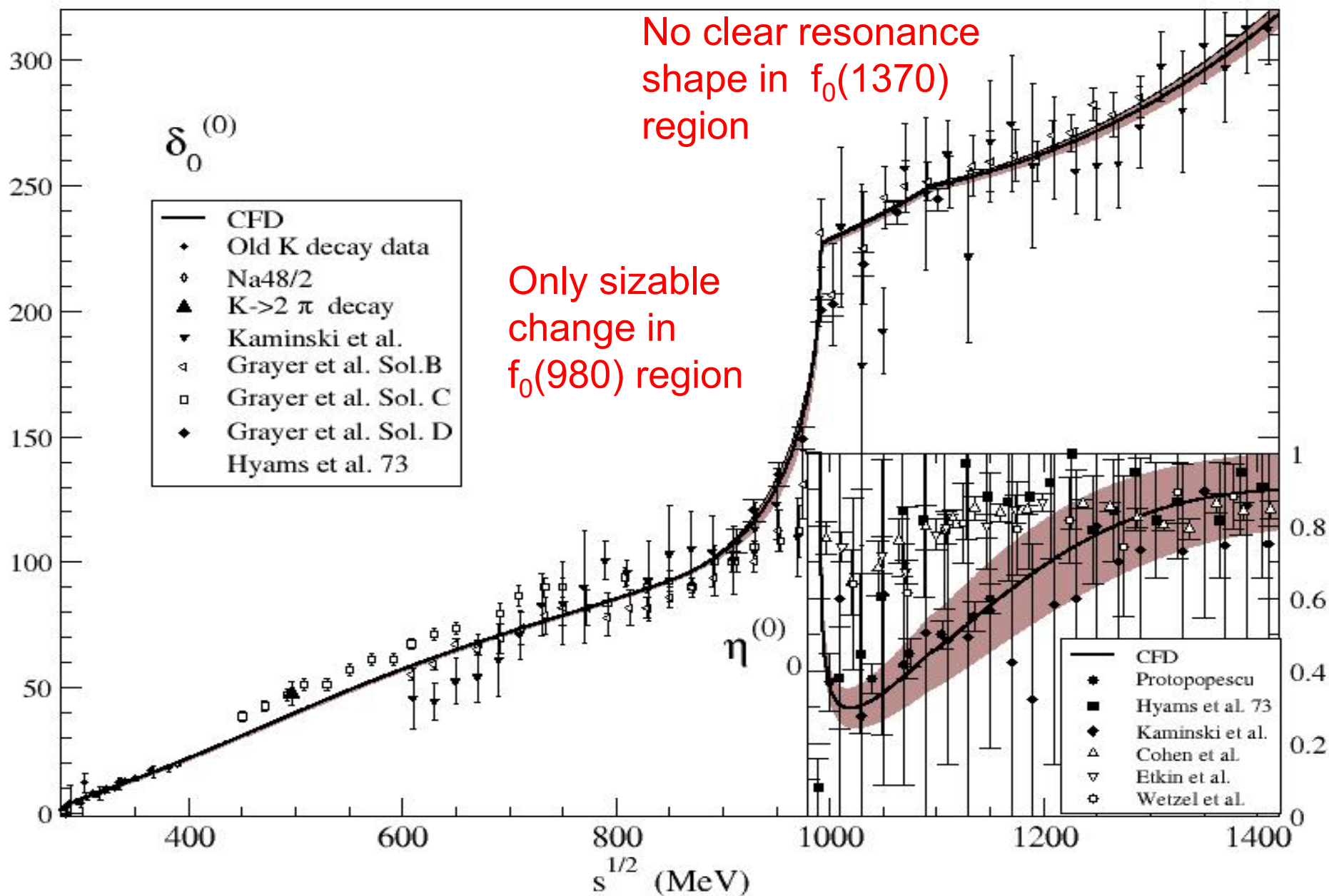
Reduced Model dependence or independence for pole determinations

We have already done this for the $\sigma/f_0(500)$, $\kappa/K_0^*(700)$
and for strange resonances below 2 GeV

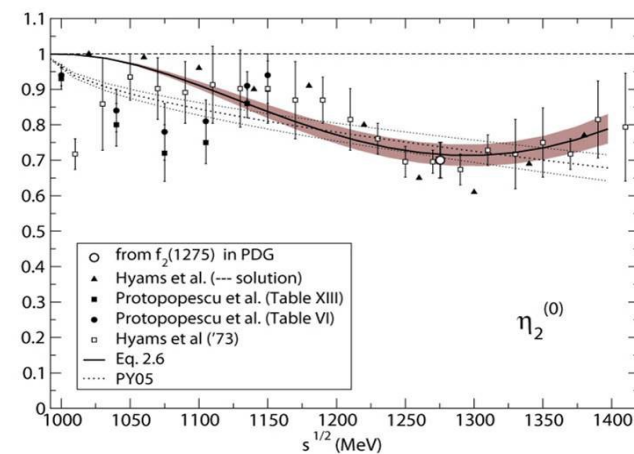
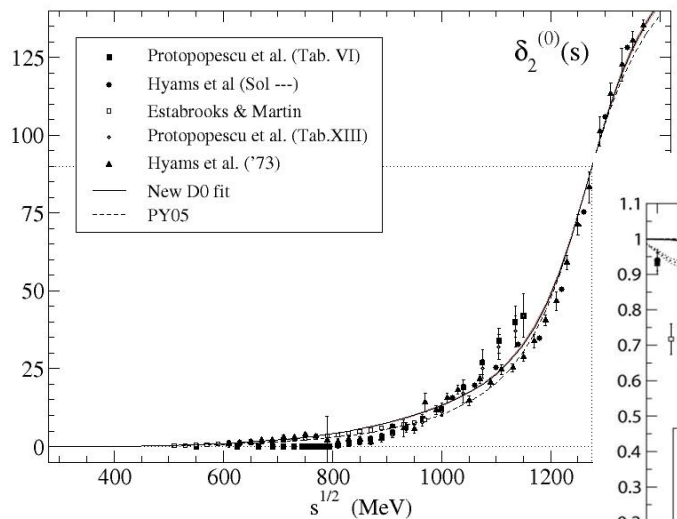
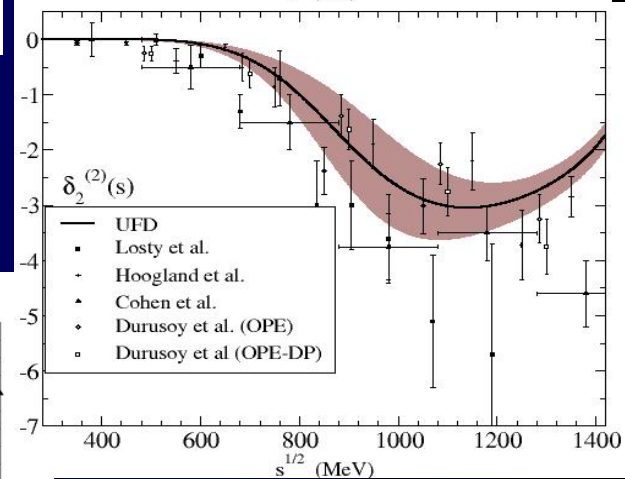
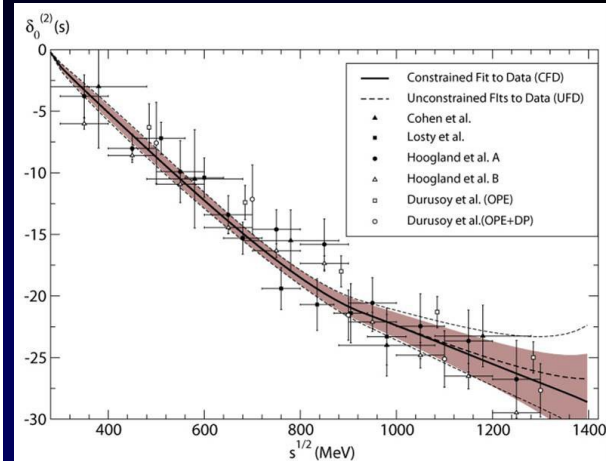
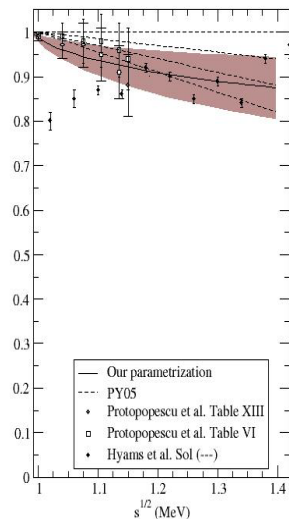
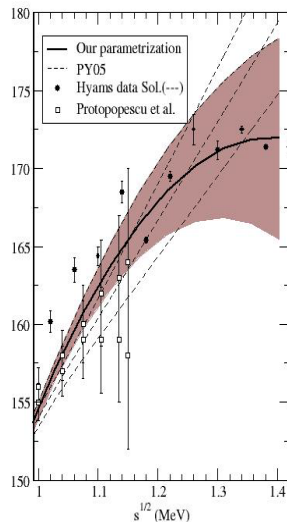
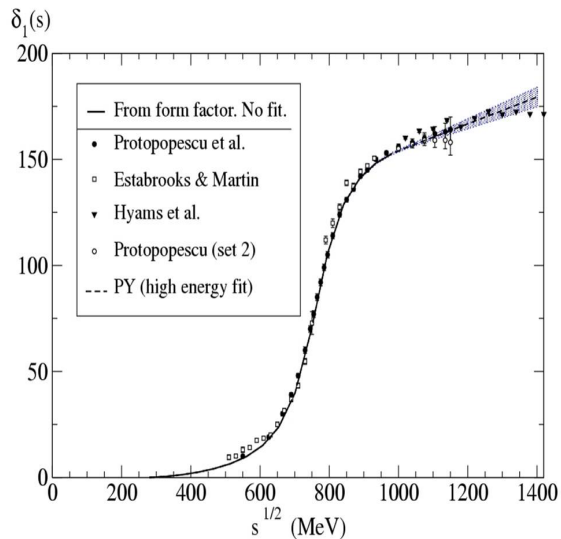
- We choose to analyze meson-meson data because it has THE MOST STRINGENT ANALYTICITY CONSTRAINTS
 - 1st Step: Unconstrained fits to data
 - 2nd Step: Check dispersion relations. Discard too bad data
 - 3rd Step: Constrained fits to data
 - 4th Step: Extract resonances with dispersive or analytic methods (This Work)

- We have already published dispersively Constrained Fits to Data (CFD):
 - $\pi\pi \rightarrow \pi\pi$ with Forward Dispersion relations and Roy equations
García Martín, Kaminski, JRP, Ruiz de Elvira, Yndurain, Phys.Rev.D 83 (2011) 074004
 - $\pi\pi \rightarrow K\bar{K}$ with Roy-Steiner Equations
JRP, A. Rodas, Eur.Phys.J.C 78 (2018) 11, 897 & Phys.Rept. 969 (2022) 1-126

$\pi\pi \rightarrow \pi\pi$ S0 wave: from unconstrained to constrained

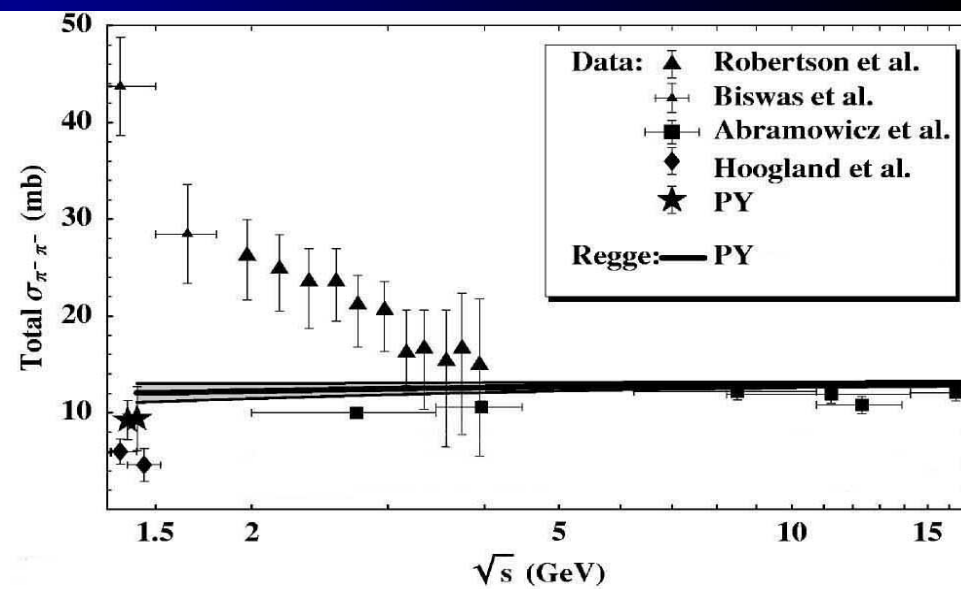
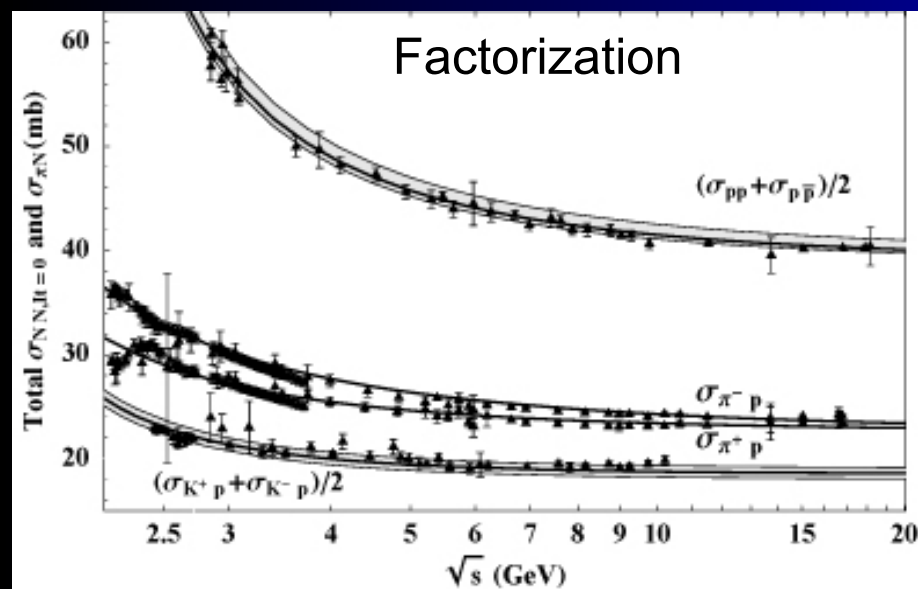
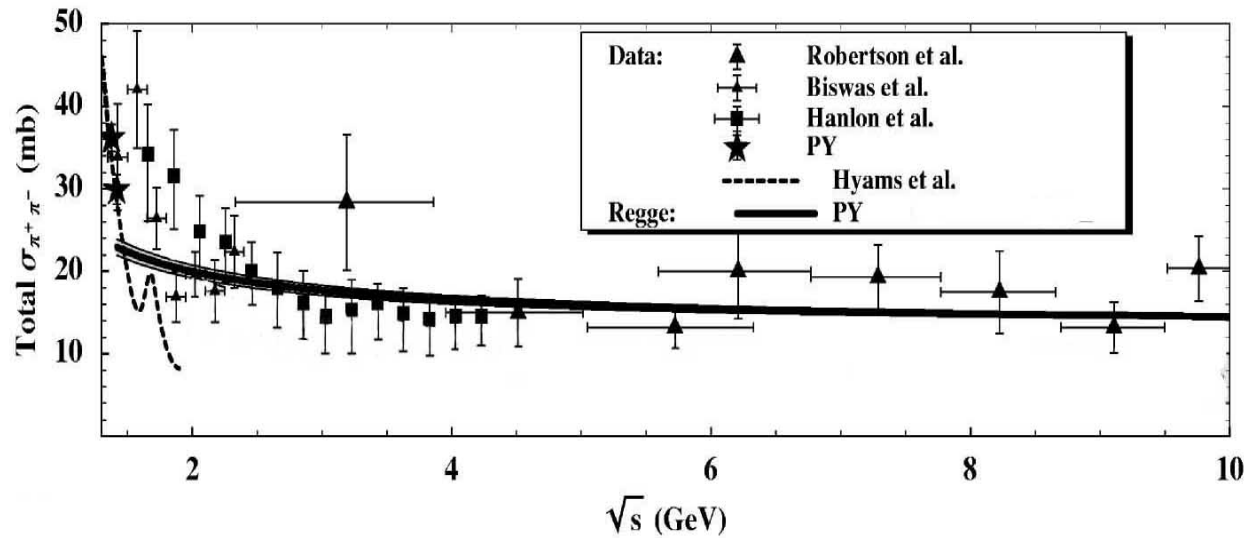
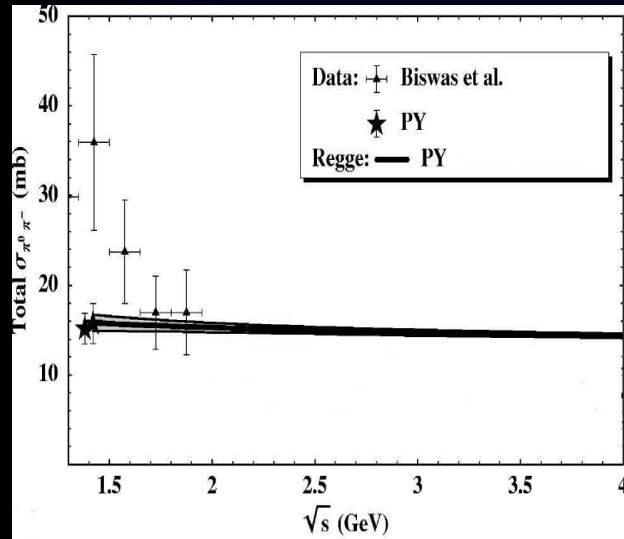


We also constrained the other $\pi\pi \rightarrow \pi\pi$ S, P, D, F waves



Detailed analysis of statistical and systematic errors

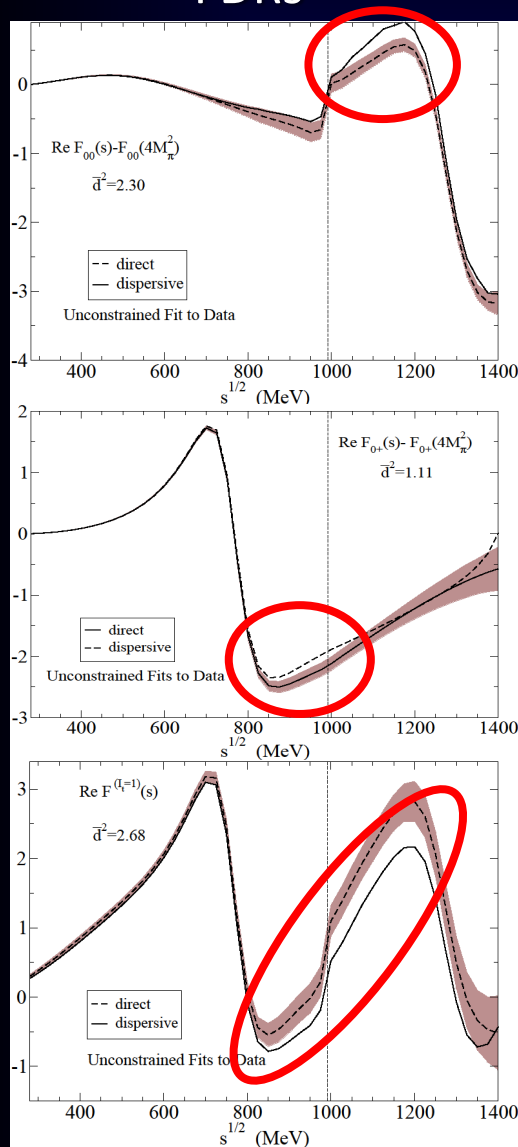
Above 1.42 GeV. Regge parametrizations of cross section data



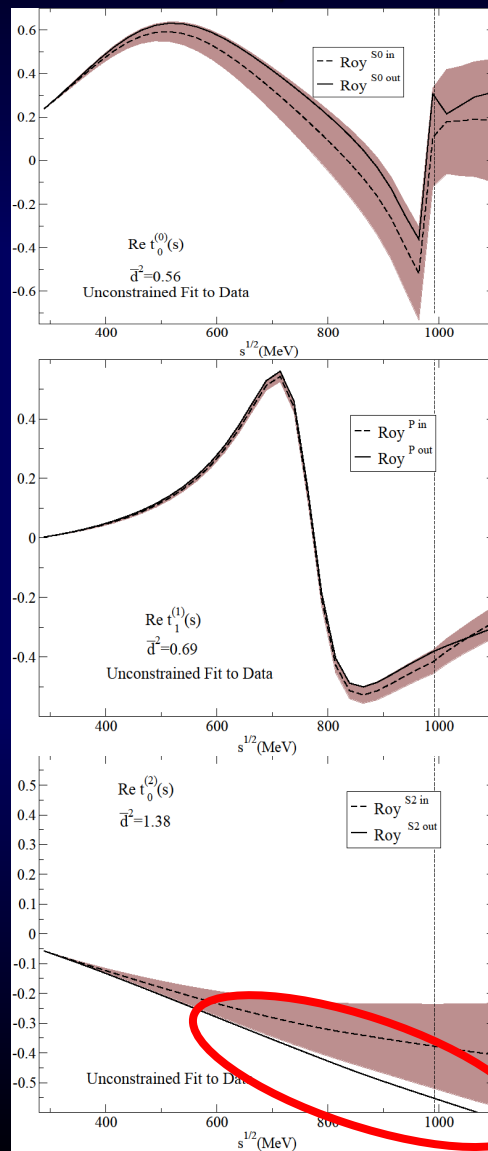
SECOND STEP: Check dispersion relations: $\pi\pi \rightarrow \pi\pi$

In general, data does not satisfy well DR. Sometimes very badly indeed

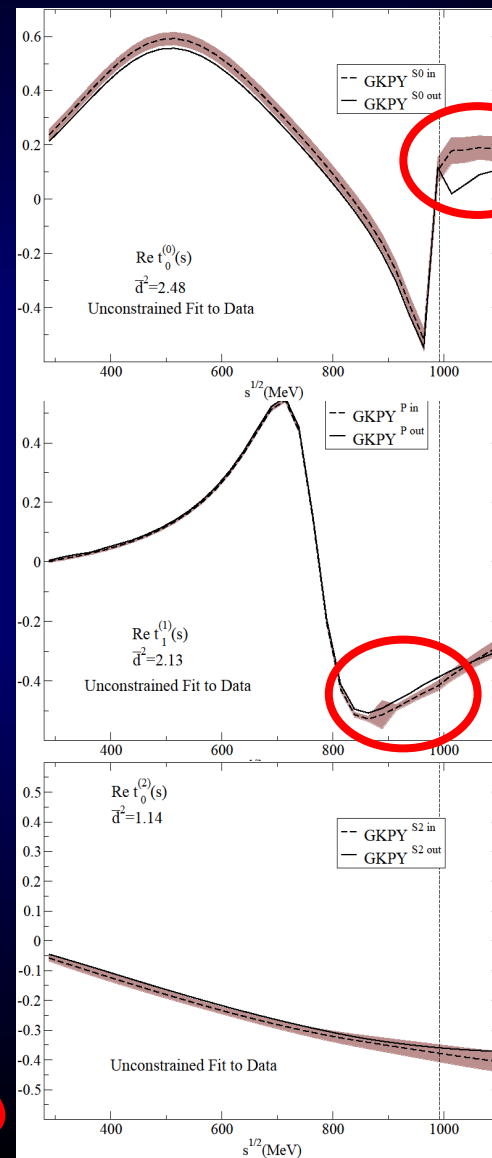
FDRs



Roy



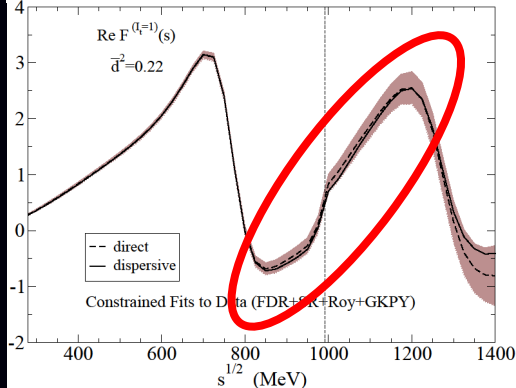
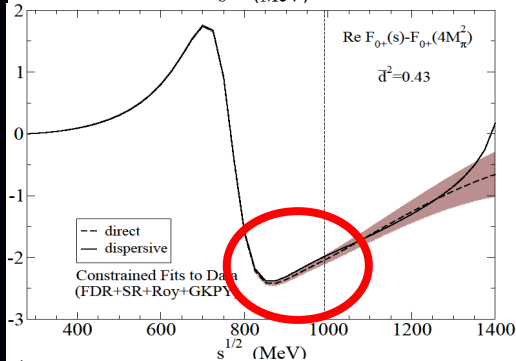
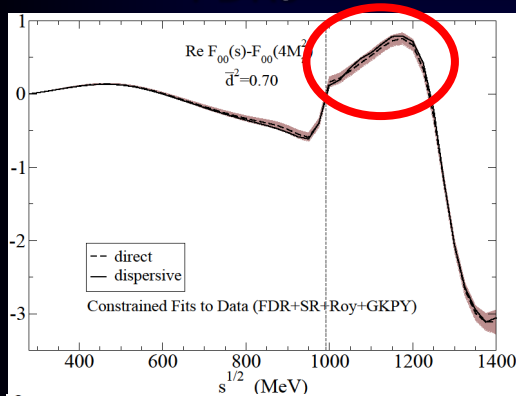
GKPY



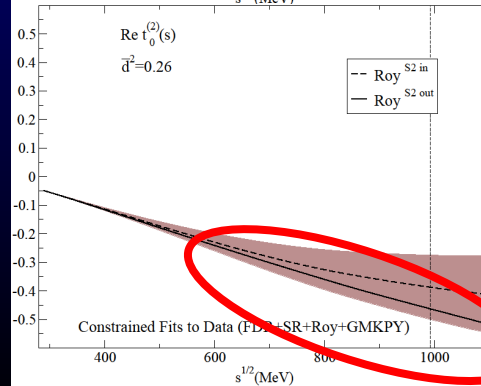
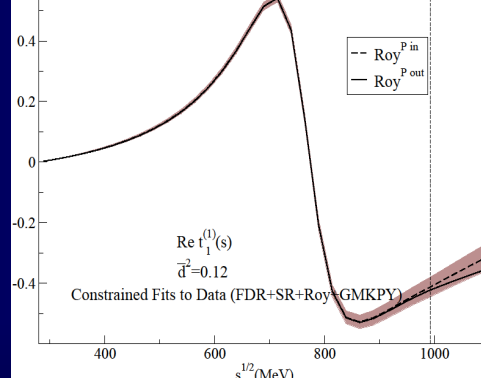
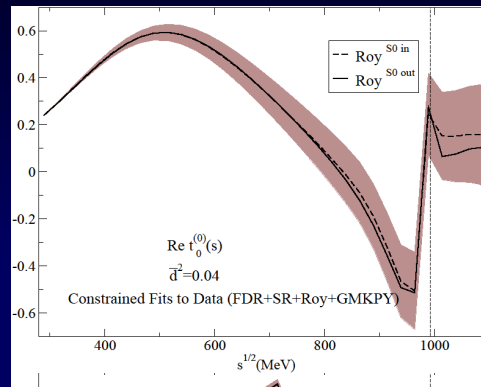
THIRD STEP: Use dispersion relations as constraints for the fits: $\pi\pi \rightarrow \pi\pi$

Very good fulfillment: Constrained Fits to Data

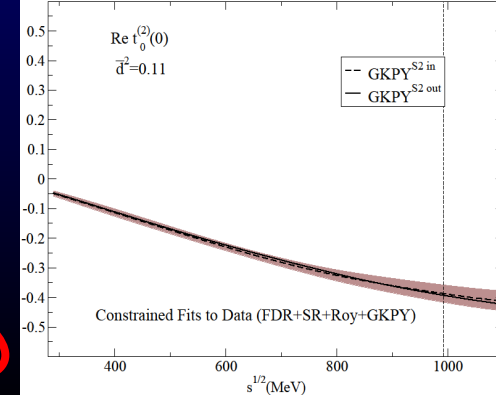
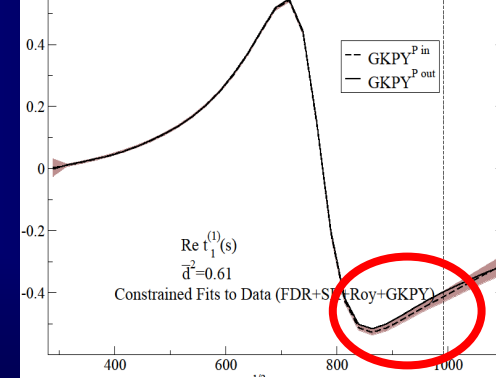
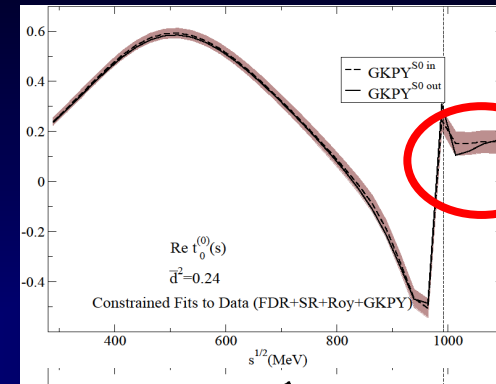
FDRs

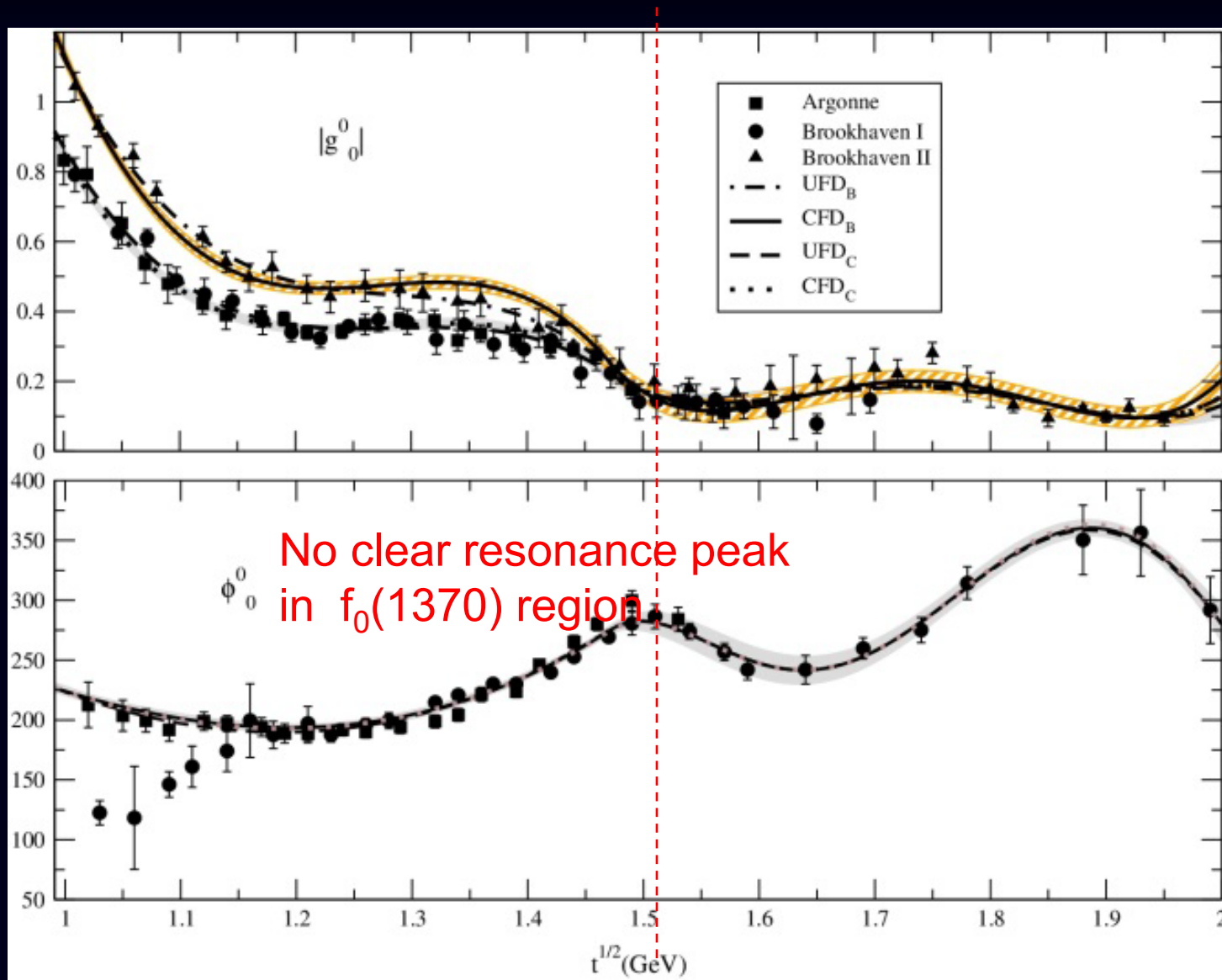


Roy



GKPY





$I=0, J=0$, Roy-Steiner eqs. Well satisfied up to 1.47 GeV

FOURTH STEP: Extract resonances from dispersive or analytic methods

Data-Driven Dispersion Relations
on amplitude or partial waves (phase+elasticity)

Model independent constraints on data description
Enhanced precision

+

Analytic methods for continuation to complex plane
avoiding specific parameterizations

Roy-like Dispersion relations provide model-independent analytic continuation to first Riemann sheet

**For elastic resonances, contiguous sheet= second sheet and $S''=1/S'$
OK for $\sigma/f_0(500)$, $\kappa/K_0^*(700)$, but NOT $f_0(1370)$,**

To reach the contiguous sheet in the inelastic case, we need an analytic continuation to the second sheet by means of general analytic functions reproducing the Dispersion Relation on the real axis or the upper-half complex plane.

Several methods in the literature:

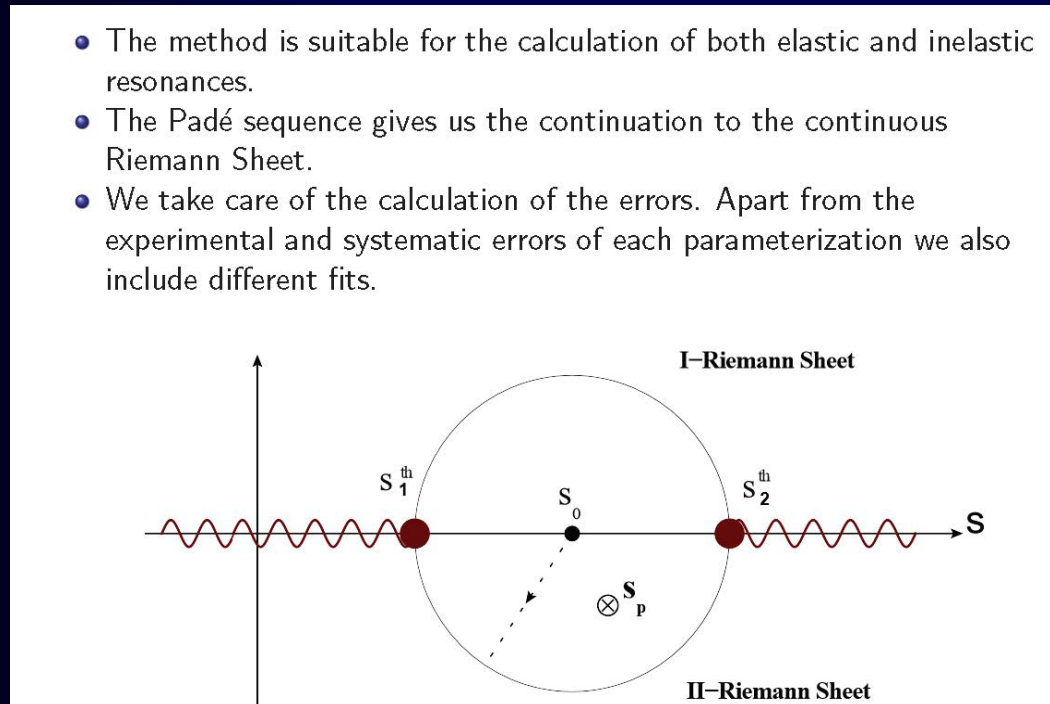
- Sequences of Padés
- Continued Fractions
- Conformal expansions
- Laurent-Pietarinen expansions
- etc...

These methods avoid specific parameterizations, have convergence theorems, etc...

Almost model independent: Does not assume any particular functional form
But requires a few derivatives. There are powerful convergence theorems
If many derivatives needed, poor convergence

Based on previous works by P.Masjuan, J.J. Sanz Cillero, I. Caprini, J.Ruiz de Elvira, JRP, A.Rodas & J. Ruiz de Elvira. Eur. Phys. J. C (2017)

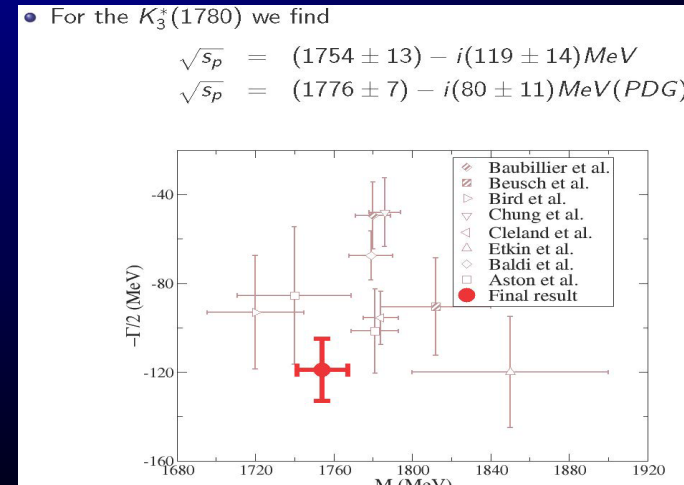
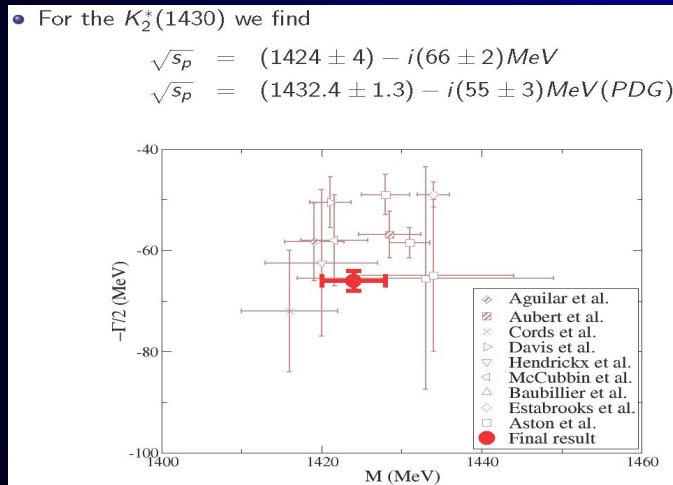
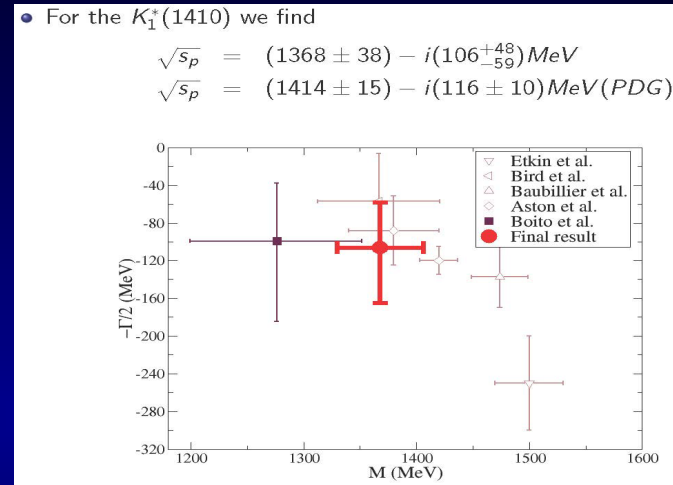
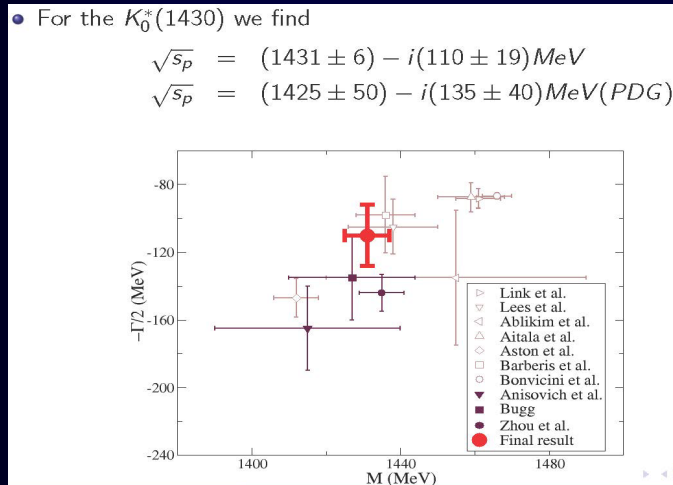
- The method is suitable for the calculation of both elastic and inelastic resonances.
- The Padé sequence gives us the continuation to the continuous Riemann Sheet.
- We take care of the calculation of the errors. Apart from the experimental and systematic errors of each parameterization we also include different fits.



CAVEAT: Requires higher order derivatives of the function to be continued

Still successfully applied to determine strange resonances from πK scattering up to 1.8 GeV

The method can be used for inelastic resonances. Provides resonance parameters WITHOUT ASSUMING SPECIFIC FUNCTIONAL FORM. We only used our constrained data fits in the real axis. Note that these are built piecewise, could be polynomials in some patches... BUT the analytic continuation was made with Padé sequences. No model



Using Padé Sequences, the kappa:

$(670 \pm 18) - i(295 \pm 28) \text{ MeV}$

Consistent with full dispersive value: $(648 \pm 7) - i(280 \pm 16) \text{ MeV}$

We now use:

$$a_0 + \frac{1}{a_1 + \frac{1}{a_2 + \frac{1}{\ddots + \frac{1}{a_n}}}}$$

Once again, no specific simple functional form assumed

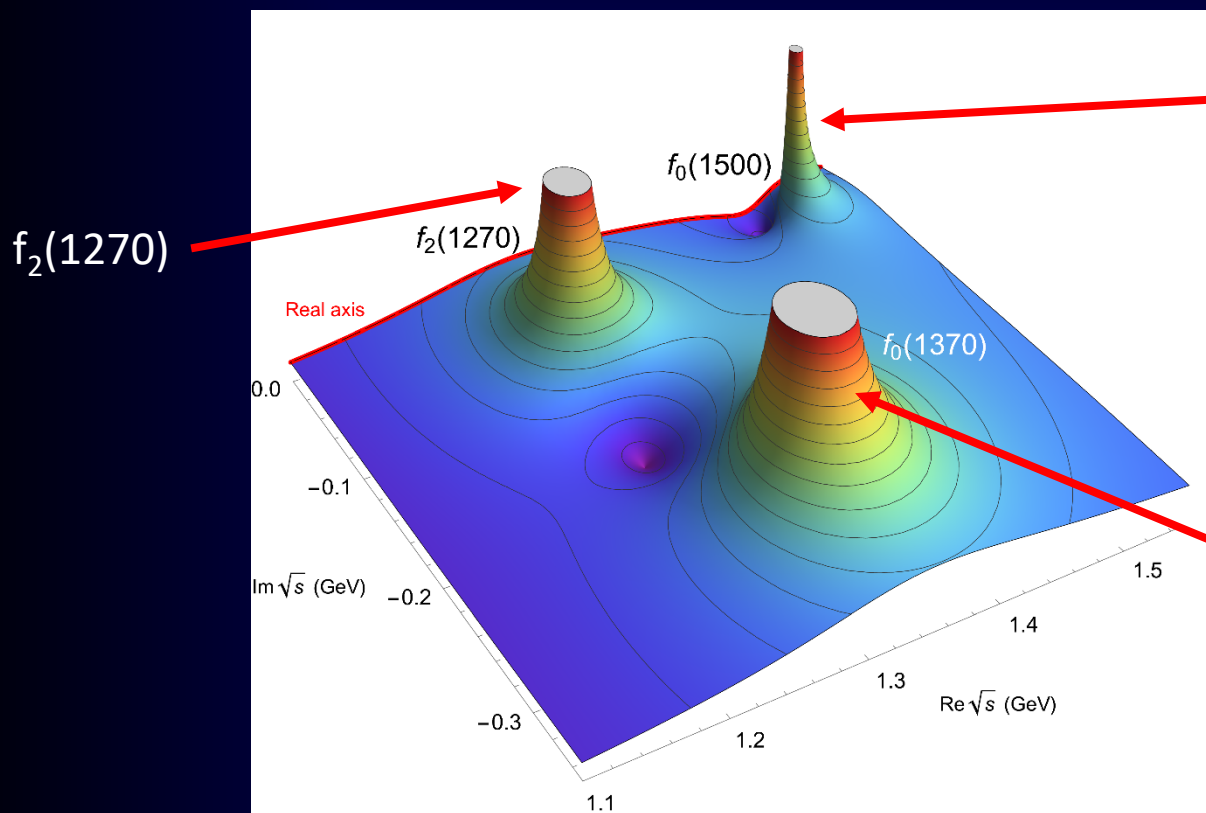
More stable and accurate than Padé, since no derivatives needed.
We have considered from 6 up to 50 terms or even more

When Padé sequences converge, perfect agreement
Actually, could be rewritten as a Padé

Roy equations applicability proof only up to 1.1 GeV. (But see later). The $f_0(1370)$ lies beyond

However, Forward Dispersion Relations applicability up to 1.42 GeV in our fits.

Complication, we see the isoscalar-wave with all spins, $J=0,2,\dots$



Even $f_0(1500)$ seen!!!,
Although not partial-wave
data used beyond 1.42 GeV
(Just a Regge description of
cross sections)

$f_0(1370)$ seen behind

Unfortunately, with just a few derivatives on the real axis, the Padé method does not converge well behind the $f_2(1270)$.

But continued fractions provide nice and stable pole description



Forward Dispersion Relations ARE SIMPLE.

Complete isospin set of 3 forward dispersion relations for :

- Two s-u symmetric amplitudes. $F_{0+} \equiv \pi^0 \pi^+ \rightarrow \pi^0 \pi^+$, $F_{00} \equiv \pi^0 \pi^0 \rightarrow \pi^0 \pi^0$
One subtraction
Only depend on two isospin states. Positivity of imaginary part

$$\operatorname{Re} F(s) - \operatorname{Re} F(4M_\pi^2) = \frac{s(s - 4M_\pi^2)}{\pi} PP \int_{4M_\pi^2}^{\infty} ds' \frac{(2s' - 4M_\pi^2) \operatorname{Im} F(s')}{s'(s' - s)(s' - 4M_\pi^2)(s' + s - 4M_\pi^2)}$$

- The $I_t=1$ s-u antisymmetric amplitude

$$\operatorname{Re} F(s) = \frac{(2s - 4M_\pi^2)}{\pi} PP \int_{4M_\pi^2}^{\infty} ds' \frac{\operatorname{Im} F(s')}{(s' - s)(s' + s - 4M_\pi^2)}$$

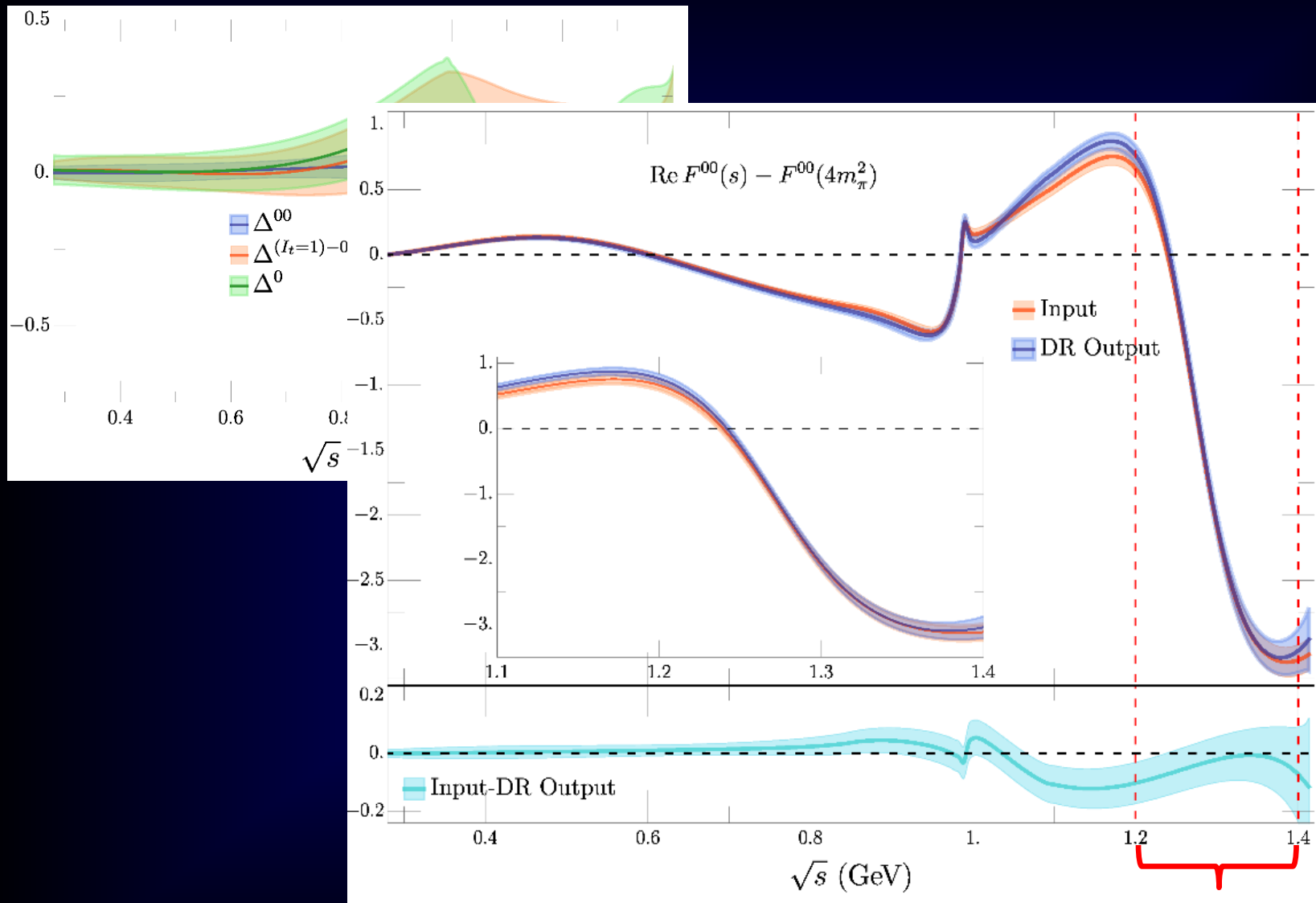
At threshold is the Olsson sum rule

Roy Eqs.

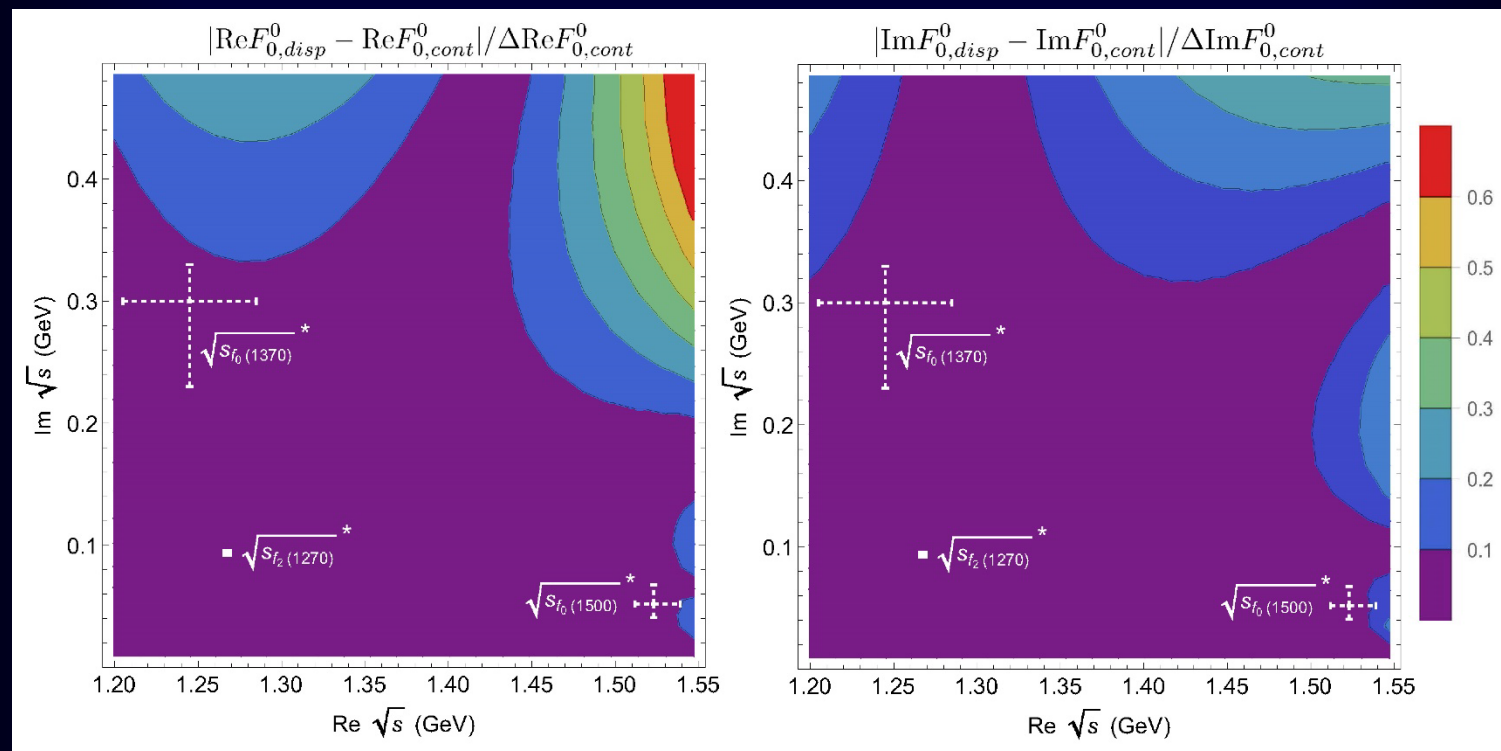
written for partial waves

MUCH MORE CUMBERSOME

There are three independent FDRs: The most precise FDR is F^{00}

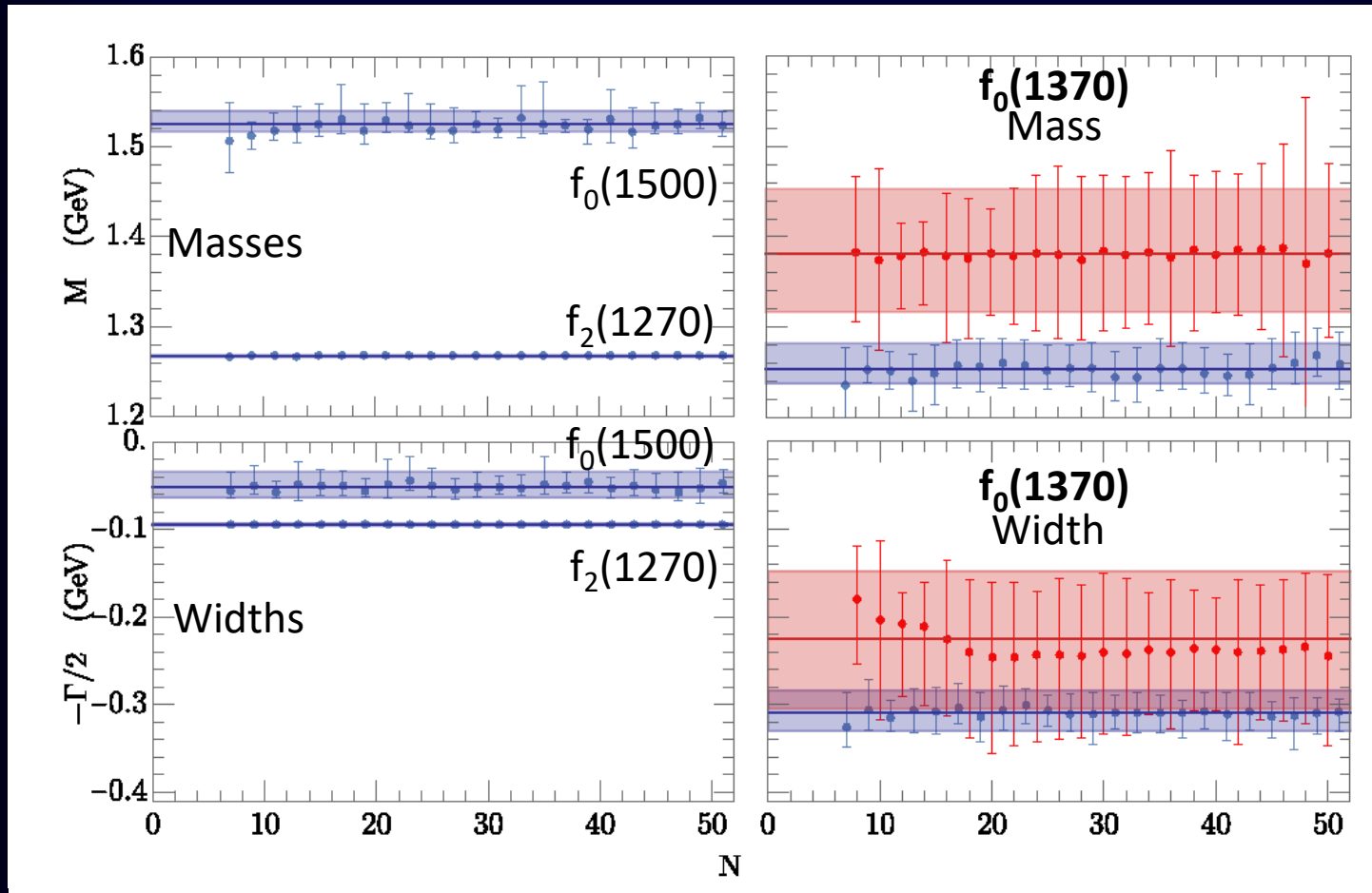


We can test how well the continued fractions fare against the FDR output in the first Riemann sheet (in the conjugated region of interest)



The difference is less than 10% of the estimated uncertainty from continued fractions
 Of course, we need the contiguous sheet in the lower-half plane. The upper-half plane is just a test.

Then we match the FDR output to continued fractions with $N=6$ to 50 and look for poles in the lower-half plane of the second sheet. We find three:

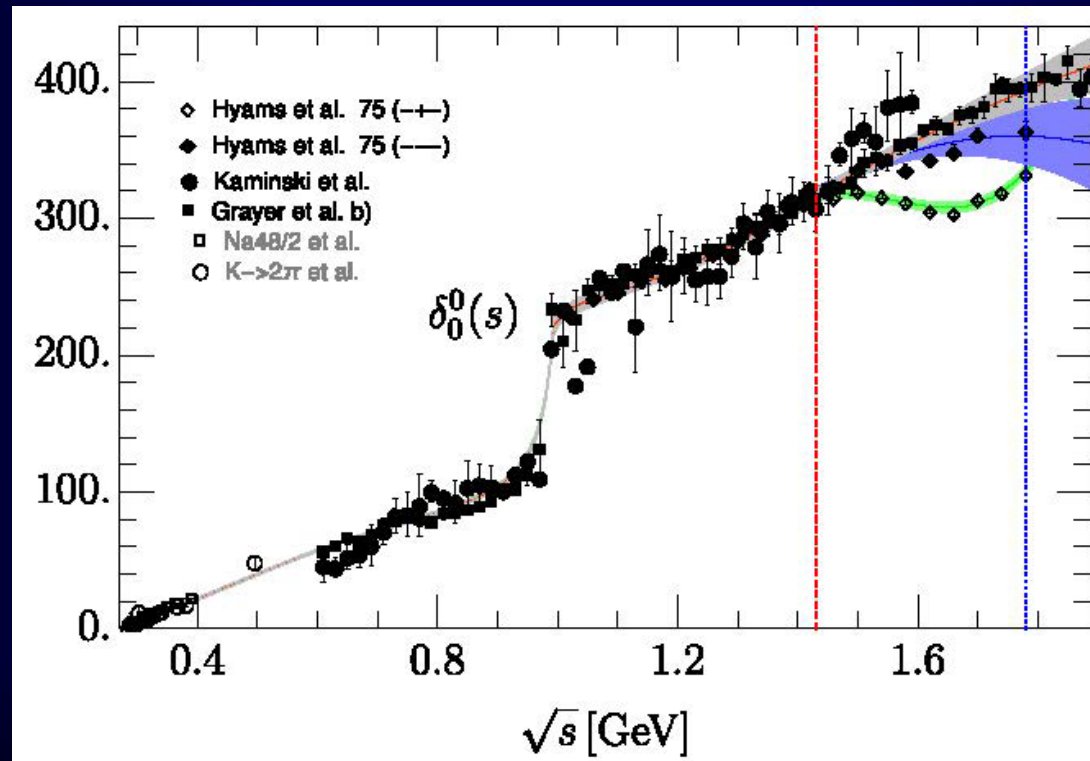


Remarkably stable against N and systematic uncertainties!

Our “old” Constrained fit to data (CFD) was a “piece-wise” function up to 1.42 GeV

Recently we have provided a “Global Fit” in terms of analytic functions, consistent with the CFD and DR up to 1.4 GeV as well as in the complex plane in the elastic region and the dispersive $\sigma/f_0(500)$ and $f_0(980)$ poles.

And continuously extended beyond 1.4 GeV to different data sets and $f_0(1500)$ scenarios



This “Global fit” is actually slightly better with respect to Dispersion Relations

For $\pi\pi$ we use both inputs

- Piece-wise Constrained fit to data (CFD)
- 3 Global “Constrained fits to data”

Method	$\sqrt{s}f_0(1370)$ (MeV)	G (GeV)
FDR+CFD+ C_N	$(1253^{+29}_{-16}) - i (309^{+21}_{-25})$	6.0 ± 0.3
FDR+Global1+ C_N	$(1232^{+29}_{-31}) - i (270^{+47}_{-32})$	4.9 ± 0.4
FDR+Global2+ C_N	$(1227^{+27}_{-22}) - i (276^{+36}_{-48})$	$4.9^{+0.4}_{-0.3}$
FDR+Global3+ C_N	$(1230^{+26}_{-21}) - i (274^{+36}_{-24})$	$4.9^{+0.4}_{-0.5}$

Our final FDR+ C_N result covers them all

$$(1245 \pm 40) - i (300^{+30}_{-70}) \quad 5.6^{+0.7}_{-1.2}$$

Further checks

- Even though Roy-like Eqs. (GKPY) not rigorously valid above 1.1 GeV, Their extrapolation is still pretty decent up to a few 100s MeV beyond.

If we extrapolate them to get the pole:

PERFECT CONSISTENCY

This confirms the scalar assignment

In addition, since $f_2(1270)$ not present in partial wave, we can use the Padé sequence Method (P_M^N) for analytic continuation.

PERFECT CONSISTENCY

Method	$\sqrt{s_{f_0(1370)}} \text{ (MeV)}$	$g_{\pi\pi} \text{ (GeV)}$
GKPY+CFD+ C_N	$(1277_{-42}^{+49}) - i (287_{-64}^{+49})$	$5.6_{-2.2}^{+2.1}$
GKPY+CFD+ P_2^N	$(1285_{-36}^{+32}) - i (219_{-44}^{+40})$	4.2 ± 0.4
GKPY+Global1+ C_N	$(1218_{-21}^{+26}) - i (218_{-32}^{+34})$	4.1 ± 1.3
GKPY+Global1+ P_1^N	$(1224_{-22}^{+31}) - i (219_{-31}^{+23})$	4.1 ± 0.4
GKPY+Global1+ P_2^N	$(1222_{-17}^{+28}) - i (214_{-21}^{+26})$	4.2 ± 0.4
Global1 param.+ C_N	$(1220_{-22}^{+27}) - i (218_{-36}^{+41})$	4.2 ± 0.4
Global1 param.+ P_1^N	$(1222_{-33}^{+39}) - i (220_{-40}^{+42})$	$4.2_{-0.8}^{+0.9}$
Global1 param.+ P_2^N	$(1219_{-27}^{+29}) - i (213_{-41}^{+43})$	3.9 ± 0.5
Global1 param.	$(1219 \pm 29) - i (214 \pm 44)$	4.16 ± 0.08

- If you want a simple analytic form consistent with data up to 2 GeV, dispersion relations up to 1.42 GeV and Roy eqs. applicability region in the complex plane, as well as the dispersive poles for $\sigma/f_0(500)$, $f_0(980)$ and this $f_0(1370)$, use our “Global fit”

Also, $f_0(1370)$ poles consistent with explicit pole in parameterization or with different analytic continuation methods

Roy-Steiner $\pi\pi \rightarrow KK$ equations applicability proved up to 1.47 GeV

Nice because they constrain the relevant S0 partial wave

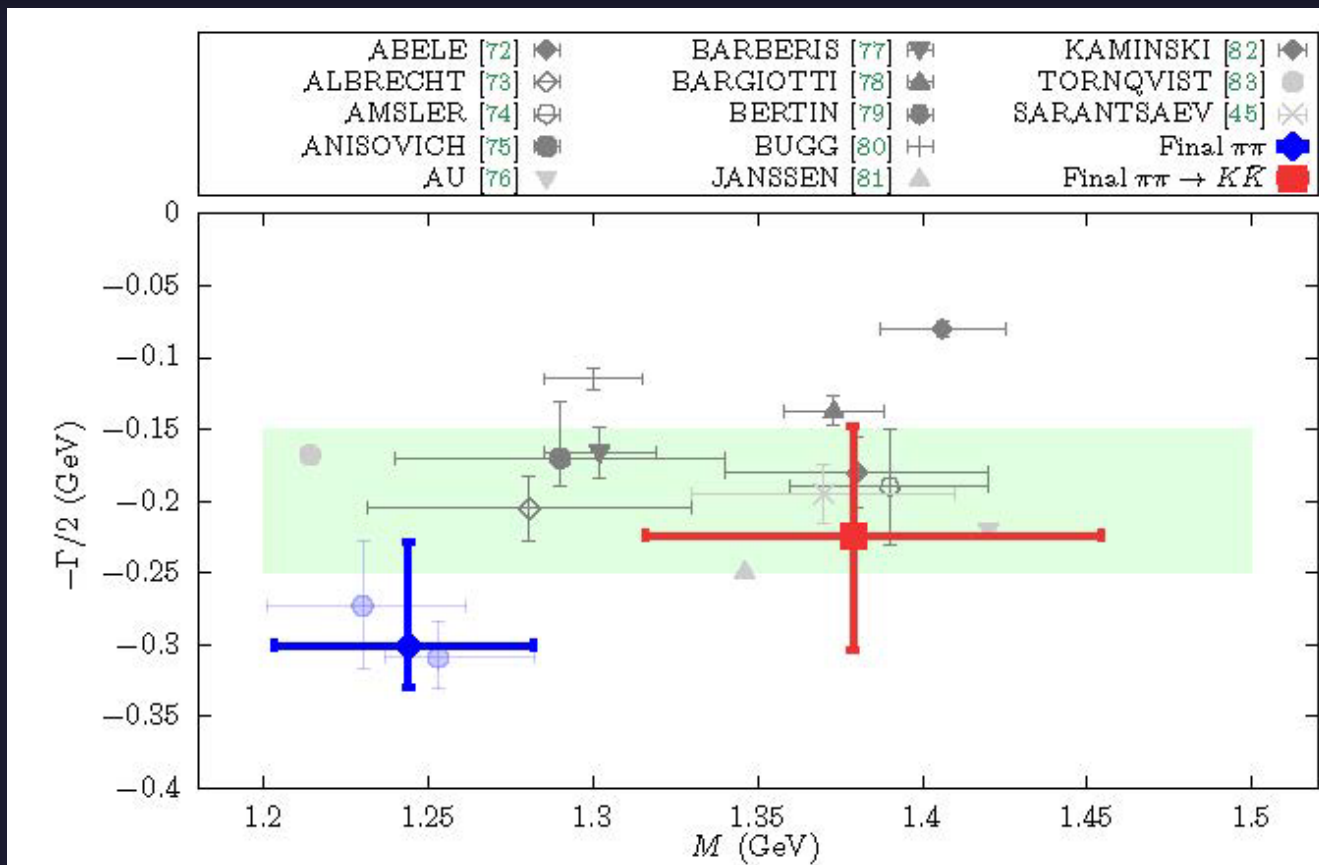
Unfortunately the $f_0(1370)$ couples even less strongly to KK

However, we always find a pole in the S0-wave around 1300 MeV, for both CFD solutions.

But large uncertainty completely dominated by choice of matching point t_m for Muskhelishvili-Omnés input in Roy-Steiner formalism.

$$\left(1380^{+70}_{-60}\right) - i \left(220^{+80}_{-70}\right) \quad 3.2^{+1.3}_{-1.1}$$

FINAL RESULTS:



$$\text{FDR}_{\pi\pi \rightarrow \pi\pi} + \text{C}_N \quad (1245 \pm 40) - i (300^{+30}_{-70}) \quad 5.6^{+0.7}_{-1.2}$$

“2σ” tension on the mass between $\pi\pi$ and KK modes

$$\text{RS}_{\pi\pi \rightarrow K\bar{K}} + \text{C}_N \quad (1380^{+70}_{-60}) - i (220^{+80}_{-70}) \quad 3.2^{+1.3}_{-1.1}$$

$\pi\pi$ -mode lighter as hinted @PDG

The very high-mass region ≈ 1500 MeV of the PDG estimate is disfavored

Summary

We aimed at reducing the model dependence of resonance determinations

- New method to determine resonance poles from data with Forward Dispersion Relations and analytic continuation techniques
(instead of the usual partial-wave dispersion relations, whose region of applicability is limited)
- Well suited for the inelastic region in $\pi\pi$ scattering, yields a pole for the $f_0(1370)$, in the low-mass, larger-width region of the present PDG estimate.
- Further consistency checks and simple parameterizations provided.
- $f_0(1370)$ pole also found in partial-wave Roy-Steiner equations from $\pi\pi \rightarrow KK$ data. Less precise than previous one and within PDG estimate.
- Small “ 2σ ” tension between the two determinations. (Already hints @ PDG)
- Given reduced model dependence this tension must be due to inconsistencies between $\pi\pi \rightarrow \pi\pi$ and $\pi\pi \rightarrow KK$ data sets.

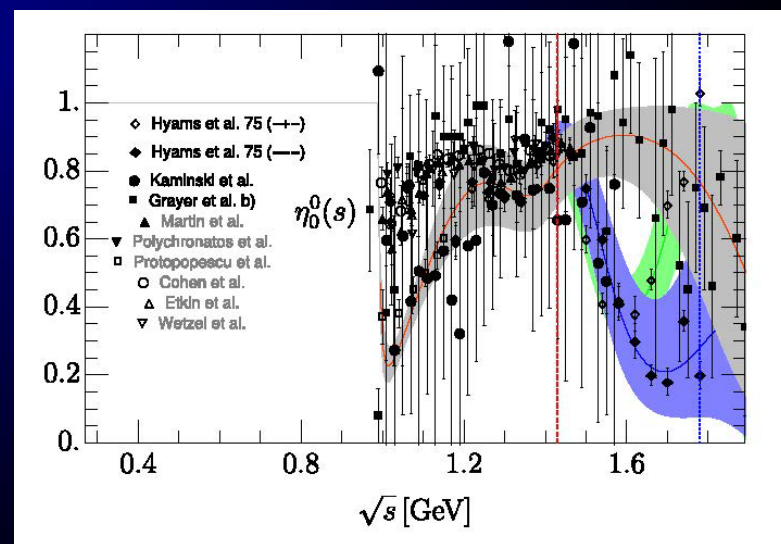
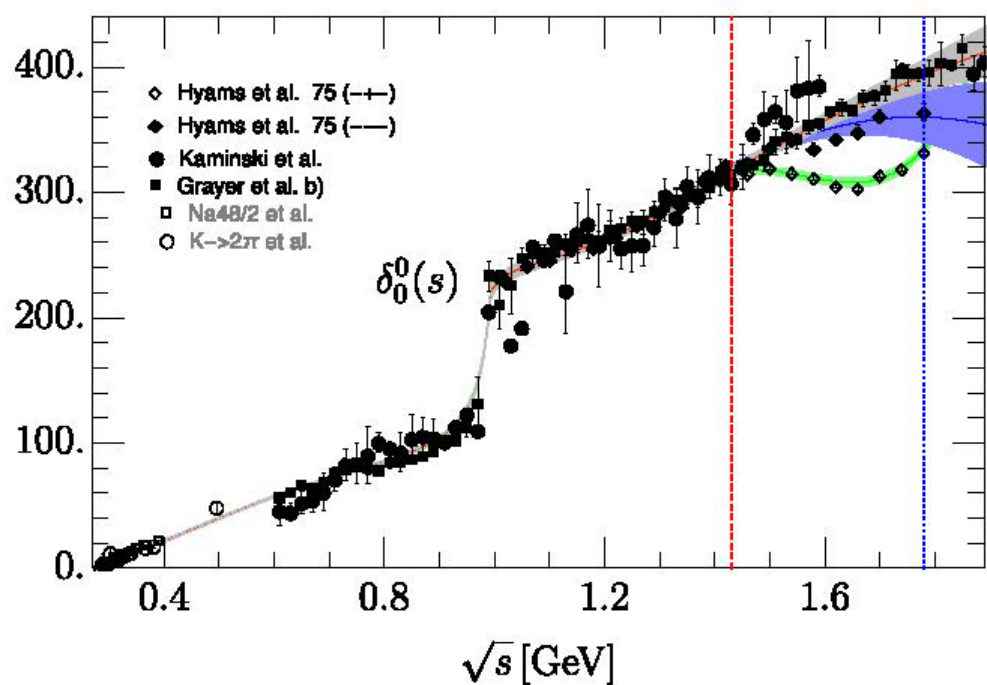
SPARE SLIDES

How the $f_0(1500)$ influences the result?

TABLE IV. Continuous fractions results using only input.

Set	$\sqrt{s_{pole}}$ (GeV)	$ g $
1	$(1.224 \pm 0.029) - i(0.217 \pm 0.042)$	4.24 ± 0.40
2	$(1.218 \pm 0.019) - i(0.219 \pm 0.036)$	4.16 ± 0.36
3	$(1.222 \pm 0.015) - i(0.221 \pm 0.024)$	4.26 ± 0.23
Final result	$(1.221^{+0.032}_{-0.026}) - i(0.219^{+0.040}_{-0.044})$	$4.22^{+0.42}_{-0.42}$

few MeV difference in pole
Depending on different data
above 1.4 GeV



$\pi\pi \rightarrow \pi\pi$ S0 wave: “Global fit” up to 2 GeV

This “Global fit” is actually slightly better with respect to Dispersion Relations

We will provide results for both

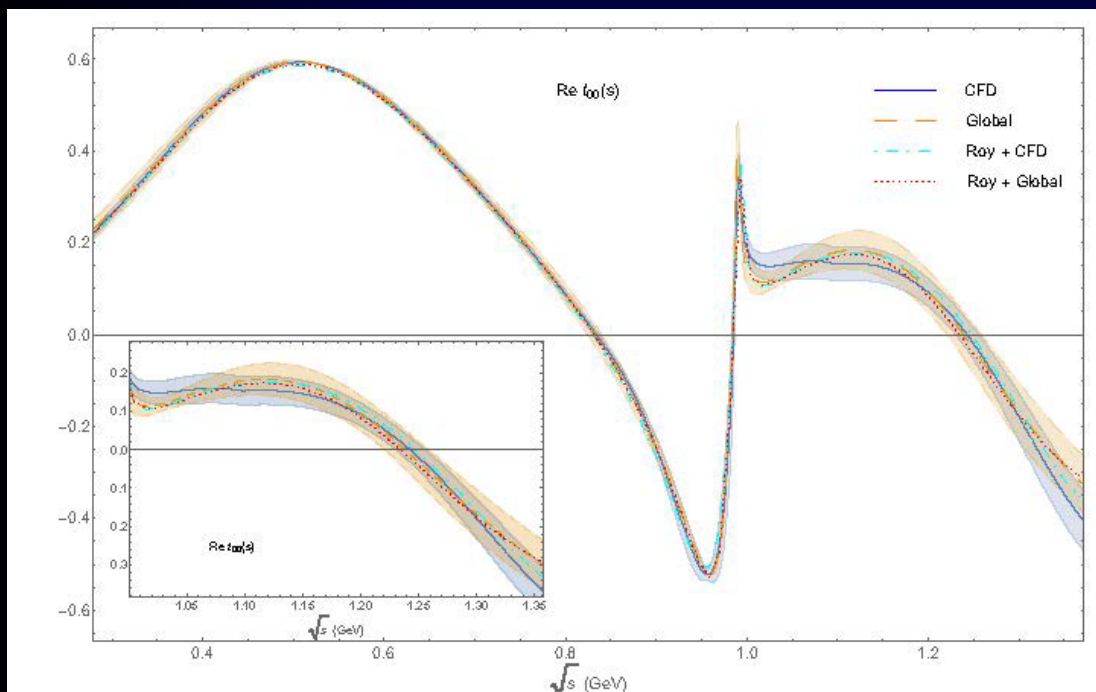


FIG. 1. Real part of the $\pi\pi$ S0 wave up to 1.35 GeV. The solid (blue) line corresponds to the piecewise CFD parameterization in [53]. Dashed (orange) curve describes solution 1 of the new Global analytic parameterization in [68]. Finally, dot-dashed (cyan) and dotted (red) lines stand for the once-subtracted Roy-equation results using as input the CFD and Global parameterizations, respectively.

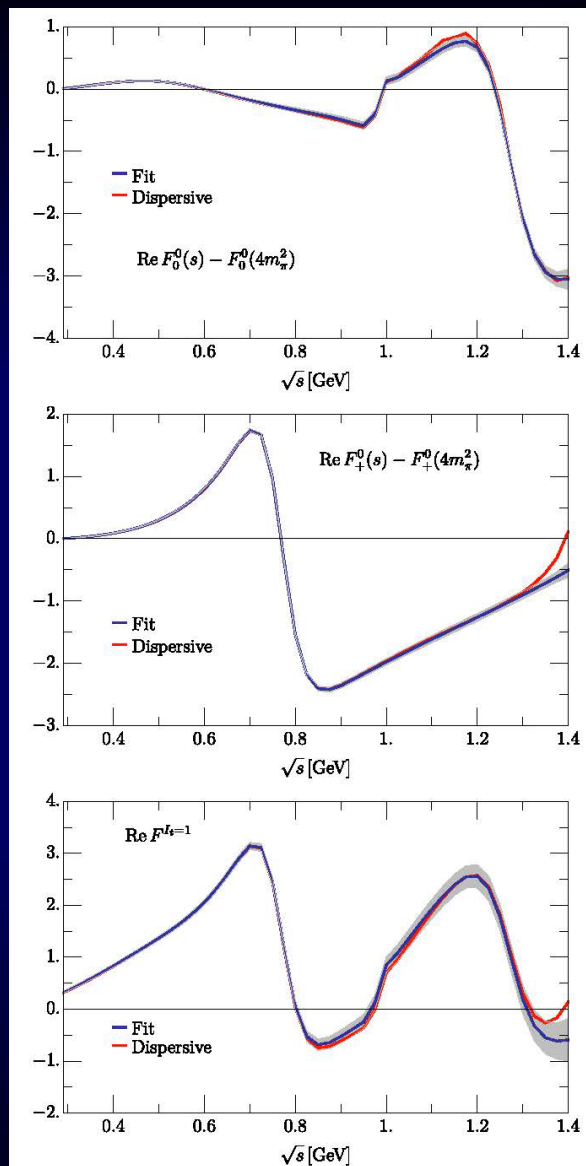


Fig. 8 Results for forward dispersion relations. Blue lines: real part coming from our new parameterizations. Orange lines: the result of the dispersive integrals. The gray bands cover the uncertainties in the difference between both. From top to bottom: a) the $\pi^0\pi^0$ FDR, b) the $\pi^0\pi^+$ FDR, c) the FDR for $l=1$ scattering

Table 5 Pole positions and $\pi\pi$ couplings of both $f_0(500)$ and $f_0(980)$ resonances from our global parameterization. Almost indistinguishable values would be obtained for solutions I, II and III. Note that they are very compatible with the GKPY dispersive results in [36]

	$\sqrt{s_{pole}}$ (MeV)	$ g $ (GeV)
$f_0(500)^{\text{GKPY}}$	$(457^{+14}_{-13}) - i(279^{+11}_{-7})$	$3.59^{+0.11}_{-0.13}$
$f_0(500)$	$(457 \pm 10) - i(278 \pm 7)$	3.46 ± 0.07
$f_0(980)^{\text{GKPY}}$	$(996 \pm 7) - i(25^{+10}_{-6})$	2.3 ± 0.2
$f_0(980)$	$(996 \pm 7) - i(25 \pm 8)$	2.28 ± 0.14

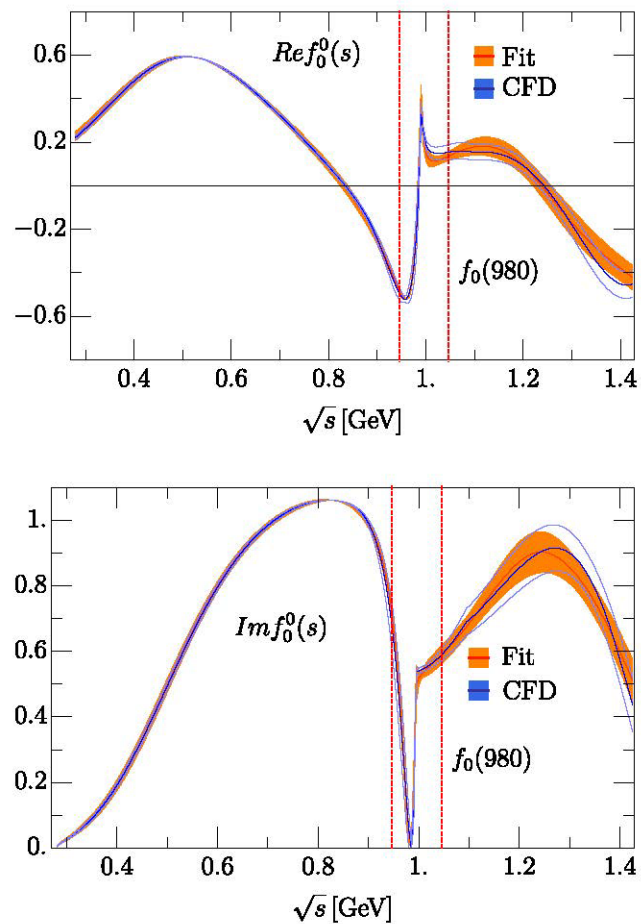
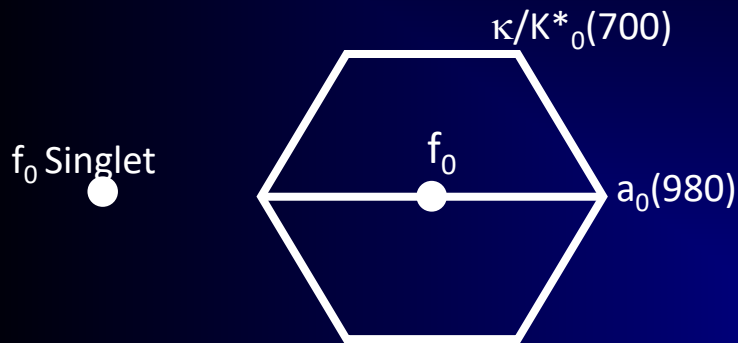


Fig. 2 Comparison between the CFD fit in [28] (blue) and solution I (Table 1, orange band). The energy region dominated by the $f_0(980)$ pole is delimited between the red dashed lines

Non-ordinary spectroscopic classification

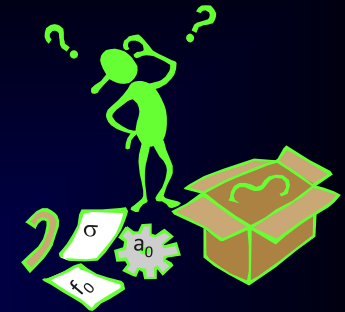
- Lightest scalar SU(3) multiplets <2 GeV. Accepted picture at RPP

Light scalar nonet <1 GeV:



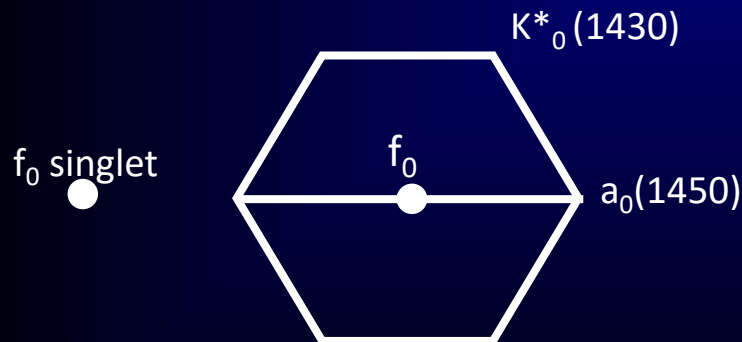
Non-strange heavier!!
Hugely Inverted $q\bar{q}$ hierarchy.
Cryptoexotics? (R.Jaffe 1976)

$\sigma/f_0(500)$ and $f_0(980)$ octet/singlet mixtures
 κ/K_0^* (700) only recently "well established at PDG"
 Only in 2021 on-line update "Needs Confirmation"



Scalar nonet >1 GeV:

One extra state $f_0(1370)$, $f_0(1500)$, $f_0(1710)$ for just one nonet above 1 GeV

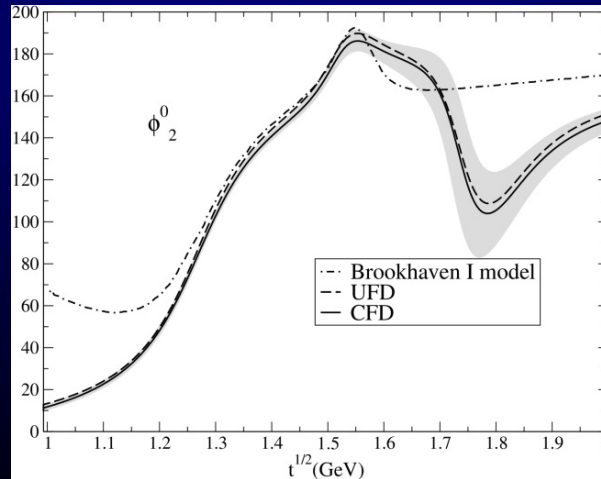
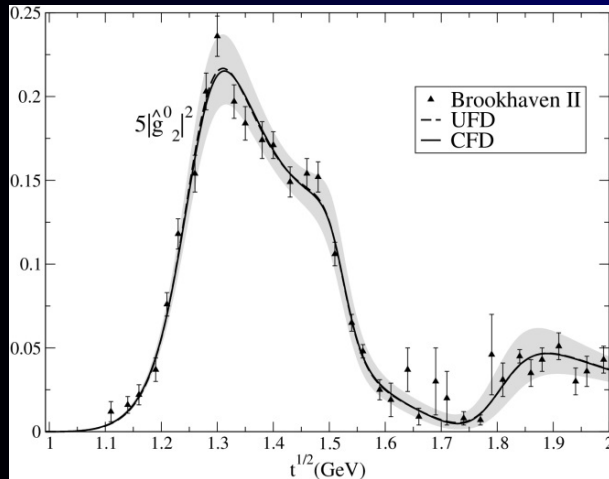
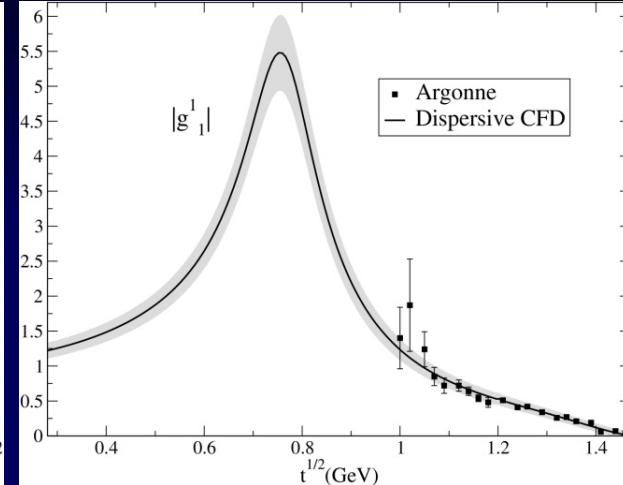
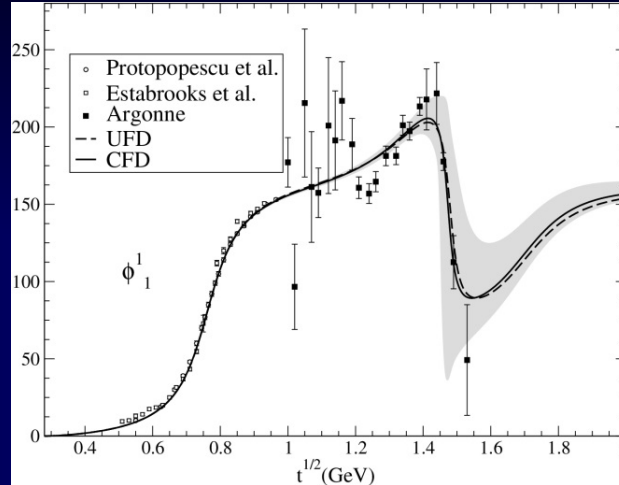
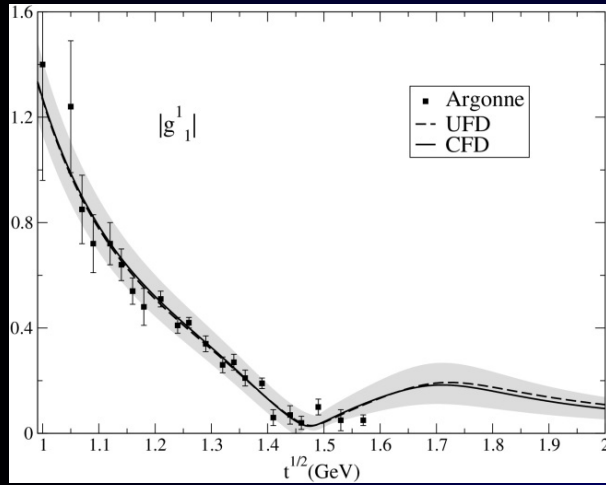


f_0 ●
 + glueball?

Also, not quite $q\bar{q}$ hierarchy

complicated mixtures
 $f_0(1370)$ worst determined and still contested
 because hard to see

Constarined SIMPLE FITS TO $\pi\pi \rightarrow KK$ DATA, including systematic uncertainties.
Other waves



UFD Inconsistent with HDR
If not constrained

$\pi K \rightarrow \pi K$ and $\pi\pi \rightarrow KK$ Hyperbolic Dispersion Relations (HDR)

$g_J^I = \pi\pi \rightarrow KK$ partial waves. We study $(I,J)=(0,0),(1,1),(0,2)$

$f_J^I = K\pi \rightarrow K\pi$ partial waves. Taken from previous dispersive study

JRP, A. Rodas PRD 2018

$$\begin{aligned}
 g_0^0(t) &= \frac{\sqrt{3}}{2} m_+ a_0^+ + \frac{t}{\pi} \int_{4m_\pi^2}^{\infty} \frac{\text{Im } g_0^0(t')}{t'(t'-t)} dt' - \frac{t}{\pi} \sum_{\ell \geq 2} \int_{4m_\pi^2}^{\infty} \frac{dt'}{t'} G_{0,2\ell-2}^0(t,t') \text{Im } g_{2\ell-2}^0(t') + \sum_{\ell} \int_{m_+^2}^{\infty} ds' G_{0,\ell}^+(t,s') \text{Im } f_{\ell}^+(s'), \\
 g_1^1(t) &= \frac{1}{\pi} \int_{4m_\pi^2}^{\infty} \frac{\text{Im } g_1^1(t')}{t'-t} dt' - \sum_{\ell \geq 2} \int_{4m_\pi^2}^{\infty} dt' G_{1,2\ell-1}^1(t,t') \text{Im } g_{2\ell-1}^1(t') + \sum_{\ell} \int_{m_+^2}^{\infty} ds' G_{1,\ell}^-(t,s') \text{Im } f_{\ell}^-(s'), \\
 g_2^0(t) &= \frac{t}{\pi} \int_{4m_\pi^2}^{\infty} \frac{\text{Im } g_2^0(t')}{t'(t'-t)} dt' + \sum_{\ell \geq 2} \int_{4m_\pi^2}^{\infty} \frac{dt'}{t'} G_{2,4\ell-2}^{0'}(t,t') \text{Im } g_{4\ell-2}^0(t') + \sum_{\ell} \int_{m_+^2}^{\infty} ds' G_{2,\ell}^{+'}(t,s') \text{Im } f_{\ell}^+(s').
 \end{aligned} \tag{39}$$

$G_{J,J}^I(t,t')$ = integral kernels, depend on a parameter
 Lowest # of subtractions. Odd pw decouple from even pw.

$$g_{\ell}^0(t) = \Delta_{\ell}^0(t) + \frac{t}{\pi} \int_{4m_\pi^2}^{\infty} \frac{dt'}{t'} \frac{\text{Im } g_{\ell}^0(t')}{t'-t}, \quad \ell = 0, 2,$$

$$g_1^1(t) = \Delta_1^1(t) + \frac{1}{\pi} \int_{4m_\pi^2}^{\infty} \frac{dt'}{t'-t} \text{Im } g_1^1(t'), \tag{40}$$

$\Delta(t)$ depend on higher waves or on $K\pi \rightarrow K\pi$.

Integrals from 2π threshold !
 "Unphysical region"

Solve in descending J order

We have used models for higher waves, but give very small contributions

$\pi\pi \rightarrow KK$ Hyperbolic Dispersion Relations (HDR)

For unphysical region below KK threshold, we used Omnés function

$$\Omega_\ell^I(t) = \exp \left(\frac{t}{\pi} \int_{4m_\pi^2}^{t_m} \frac{\phi_\ell^I(t') dt'}{t'(t'-t)} \right),$$

$$\Omega_\ell^I(t) \equiv \Omega_{\ell,R}^I(t) e^{i\phi_\ell^I(t)\theta(t-4m_\pi^2)\theta(t_m-t)},$$

This is the form of our HDR: Roy-Steiner+Omnés formalism

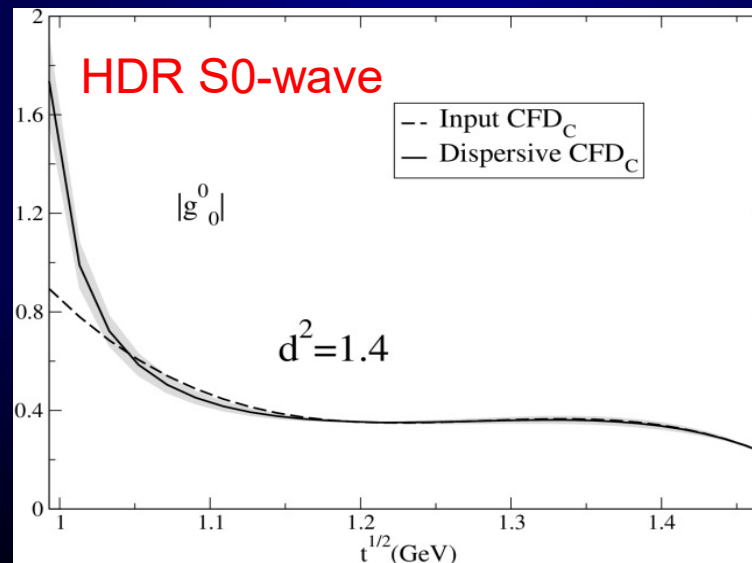
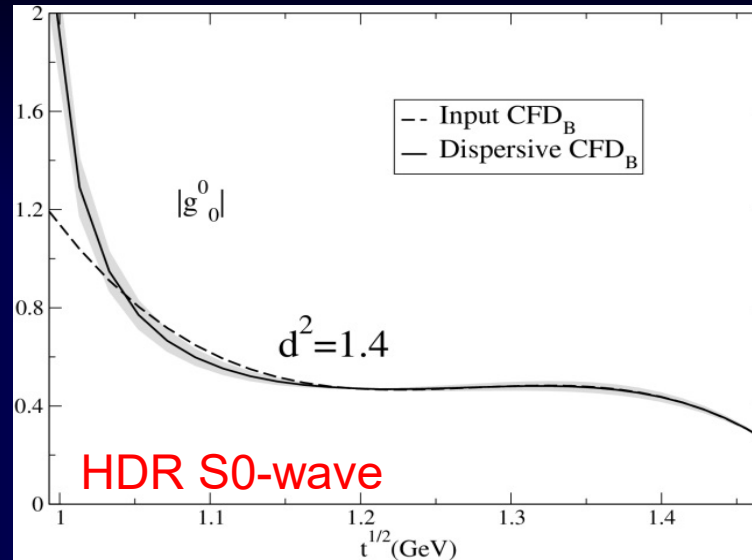
$$g_0^0(t) = \Delta_0^0(t) + \frac{t\Omega_0^0(t)}{t_m-t} \left[\alpha + \frac{t}{\pi} \int_{4m_\pi^2}^{t_m} dt' \frac{(t_m-t')\Delta_0^0(t') \sin \phi_0^0(t')}{\Omega_{0,R}^0(t')t'^2(t'-t)} + \frac{t}{\pi} \int_{t_m}^{\infty} dt' \frac{(t_m-t')|g_0^0(t')| \sin \phi_0^0(t')}{\Omega_{0,R}^0(t')t'^2(t'-t)} \right]$$

$$g_1^1(t) = \Delta_1^1(t) + \Omega_1^1(t) \left[\frac{1}{\pi} \int_{4m_\pi^2}^{t_m} dt' \frac{\Delta_1^1(t') \sin \phi_1^1(t')}{\Omega_{1,R}^1(t')(t'-t)} + \frac{1}{\pi} \int_{t_m}^{\infty} dt' \frac{|g_1^1(t')| \sin \phi_1^1(t')}{\Omega_{1,R}^1(t')(t'-t)} \right],$$

$$g_2^0(t) = \Delta_2^0(t) + t\Omega_2^0(t) \left[\frac{1}{\pi} \int_{4m_\pi^2}^{t_m} dt' \frac{\Delta_2^0(t') \sin \phi_2^0(t')}{\Omega_{2,R}^0(t')t'(t'-t)} + \frac{1}{\pi} \int_{t_m}^{\infty} dt' \frac{|g_2^0(t')| \sin \phi_2^0(t')}{\Omega_{2,R}^0(t')t'(t'-t)} \right].$$

We can now check how well these HDR are satisfied

**Dominant source
of error for $f_0(1370)$**

Two possible solutions for S_0 wave

Constrained fits
are consistent with
Roy Steiner Eqs.